J Bone Miner Metab (2001) 19:267–276

Journal of
Bone and
Mineral
Metabolism

Original articles

Histochemical examination of osteoblastic activity in op/op mice with or without injection of recombinant M-CSF

Ikuko Nishino[1], Norio Amizuka[2], and Hidehiro Ozawa[3]

[1] Department of Physical Therapy, School of Health Science, Niigata University of Health and Welfare, Niigata, Japan
[2] Department of Oral Anatomy, Niigata University Faculty of Dentistry, Niigata, Japan
[3] Institute for Dental Science, Matsumoto Dental University, 1780 Gobara, Hirooka, Shiojiri 399-0704, Japan

Abstract Osteopetrotic (op/op) mice do not exhibit bone remodeling because of defective osteoclast formation caused by the depletion of macrophage colony-stimulating factor (M-CSF). In the present study, we investigated tibial bones of op/op mice with or without prior injections of M-CSF to determine whether osteoclast formation and subsequent bone resorption could activate osteoblasts, which is known as a "coupling" phenomenon. In op/op mice, no osteoclasts were present, but the metaphyseal osteoblasts adjacent to the growth plate cartilage seemed to be active, revealing an intense alkaline phosphatase (ALPase) immunoreactivity. Consequently, primary trabecular bones were extended continuously to the diaphysis, indicating that bone modeling is well achieved in op/op mice. In contrast with the metaphysis, most of the diaphyseal osteoblasts were flattened and showed weak ALPase activity, and, as a result, they seemed to be less active. Osteopontin (OPN) was localized slightly at the interface between bone and cartilage matrices of the primary trabeculae. In contrast, in op/op mice injected with M-CSF, tartrate-resistant acid phosphatase-positive osteoclasts appeared, resorbing trabecular bones of the diaphyseal region. The diaphyseal osteoblasts in the vicinity of the active osteoclasts were cuboidal and exhibited strong ALPase immunoreactivity. OPN was observed not only at the bone–cartilage interface, but also significantly on the resorption lacunae beneath the bone-resorbing osteoclasts. These observations indicate that the activation of diaphyseal osteoblasts appears to be coupled with osteoclast formation and subsequent osteoclastic bone resorption. Alternatively, the metaphyseal osteoblasts at the chondro–osseous junction seemed to be less affected by osteoclastic activity.

Key words osteoblast · op/op mouse · coupling factor · osteoclast · osteopontin

Offprint requests to: H. Ozawa
Received: January 9, 2001 / Accepted: April 9, 2001

Introduction

Bones undergo modeling or remodeling by deposition and resorption to retain their physiological strength and turnover of bone materials [1–4]. These processes appear to be regulated by an interaction between osteoclasts and osteoblasts. Baron et al. divided "remodeling" into five morphological stages: quiescence, activation, resorption, reversal and formation [5]. In the quiescence phase, osteoblasts have a flat shape, lower bone-forming ability and are called bone–lining cells [6]. During the activation phase, preosteoclasts differentiate into multinucleated osteoclasts by direct contact with osteoblastic interstitial cells and are activated following stimulation by hormones and cytokines, including parathyroid hormone, 1,25-dihydroxyvitamin D_3, prostaglandin E, interleukins, tumor necrosis factors, transforming growth factors (TGFs), and osteoclast differentiation factor (ODF)/osteoprotegerin ligand (OPGL) [7–10] . During the resorption phase, activated osteoclasts secrete acid phosphatase (ACPase) and hydrolases to decompose inorganic and organic material and form resorption lacunae, which will become future reversal lines [5,11,12]. Of importance is the possibility that osteoclastic bone resorption triggers differentiation and activation of osteoblasts during the reversal phase, which is referred to as a "coupling" phenomenon [13]. During the formation phase, active osteoblasts secrete bone matrices, and ACPase-positive cement lines are formed between newly formed bone and old bone matrices [5,14].

Howard et al. proposed the existence of a "coupling factor" between bone resorption and formation, which would be released during osteoclastic resorption to osteoblastic activation [15]. Although the existence of this coupling factor has not been validated, there are some candidates, such as bone morphogenetic proteins (BMPs), and TGF-β. Cement lines and the lamina limitans are osteopontin (OPN) rich and have an

Arg-Gry-Asp (RGD) motif that has the ability to bind to osteoclastic integrin αvβ3 [16]. OPN is secreted by osteoblasts and osteoclasts [17–20], and its accumulation in the cement lines has led to the proposal of a putative function for OPN of attaching newly secreted bone matrices, which is bone remodeling. Therefore, OPN may play an important role in the cellular coupling between osteoclasts and osteoblasts.

The op/op mouse is a mutant animal model that presents with osteopetrosis due to macrophage colony-stimulating factor (M-CSF) deficiency. The bone abnormality in op/op mice is caused by a failure of osteoclast differentiation [21–24]. The injection of recombinant human (rh) M-CSF has proved to be successful for the induction of osteoclasts and rescue of osteopetrosis [25–28]. However, it has not been demonstrated whether osteoclast induction is able to influence the activation of osteoblasts. Notwithstanding, coupling is the essential phenomenon of bone turnover, but morphological analysis of coupling in normal animals appears to be difficult due, in part, to a complex environment, including systemic hormones, local factors, blood vessels, and mechanical stress. To avoid these complexities, including the effects of osteoclasts, we first used op/op mice to examine osteoblasts in the absence of osteoclasts, and then redid the same experiments in op/op mice in which osteoclasts had been induced by prior M-CSF injection. The aim of the present study was to histologically define the "coupling phenomenon" and to demonstrate the activity of osteoblasts with or without osteoclastic bone resorption.

Materials and methods

Treatment with rhM-CSF

F_2 homozygotes (op/op) mice were raised from breeding pairs of B6C3F1-a/a heterozygotes (op/+) mice obtained from the Jackson Laboratory (Bar Harbor, ME, USA). The op/op mice were distinguished by failure of incisor rupture and skull deformation at 10 days of age, according to Marks and Lane [29]. Mice were treated with a single peritoneal injection of 5μg rhM-CSF (Morinaga Milk Industry, Kanagawa, Japan) move 11 days after birth. As a control experiment, phosphate-buffered saline (PBS) was injected into mice instead of rhM-CSF. Mice were killed 5 days after injection, and the tibiae were extracted.

Tissue preparation and immunohistochemitry for OPN and alkaline phosphatase

Animals were perfused through the left ventricle with 4% paraformaldehyde in 0.1 M phosphate buffer (pH 7.4) under diethylether anesthesia, and the tibiae were removed. Specimens were immersed in the same fixative for 4 h at 4°C, and then decalcified with 4.13% EDTA for 4 days at 4°C. Specimens were dehydrated with increasing concentrations of ethanol and were embedded in paraffin. For OPN and alkaline phosphatase (ALPase) immunodetection, dewaxed paraffin sections were treated with 0.1% hydrogen peroxidase for 15 min for the inhibition of endogenous peroxidase, and were subsequently preincubated with 1% bovine serum albumin in PBS (BSA-PBS; pH 7.4) for 30 min at room temperature. Sections were incubated with rabbit antiOPN (at a dilution of 1:200), or rabbit antiALPase (at a dilution of 1:100) prior to incubation with a secondary antibody against rabbit IgGs, as reported previously [30]. For double staining with tartrate-resistant acid phosphatase (TRACPase), immunostained sections were incubated in a solution as follows: the antiserum to OPN was raised in rabbits against a synthetic peptide having the amino acid sequence Glu-Gln-Tyr-Pro-Asp-Ala-Thr-Asp-Glu-Asp-Leu-Thr-Ser-Arg-Met-Lys, corresponding to the hydrophilic residues from the N-terminal region of rat OPN [31].

Histochemistry for TRACPase

Paraffin sections with or without immunostaining were used for the detection of TRACPase as reported previously [32]. In brief, the sections were incubated in a mixture of 8 mg of naphthol AS-BI phosphate (Sigma, St. Louis, MO, USA), 70 mg of red violet LB salt (Sigma) and 50 mM L(+) tartaric acid (0.76 g, Nacalai Tesque, Kyoto, Japan) diluted in 0.1 M sodium acetate buffer (pH 5.0) for 20 min at 37°C.

Ultrastructural studies

The mice were perfused with a mixture of 2% paraformaldehyde and 2.5% glutaraldehyde in 0.067 M cacodylate buffer through the left ventricles under diethylether anesthesia. The tibiae of each mouse were extracted and immersed in the same fixative for approximately 24 h at 4°C. Some specimens were decalcified with 4.13% EDTA solution prior to postfixation. All specimens were postfixed with 1% OsO4 in 0.1 M cacodylate buffer (pH 7.4) containing 1.5% ferrocyanide for 2 h at 4°C. The specimens were dehydrated with ascending concentrations of acetone and embedded in Epoxy resin (Polysciences, Warrington, PA, USA) prior to observation using a transmission electron microscope (TEM) JEM-100CX II (JOEL, Tokyo, Japan) operated at 80 kV.

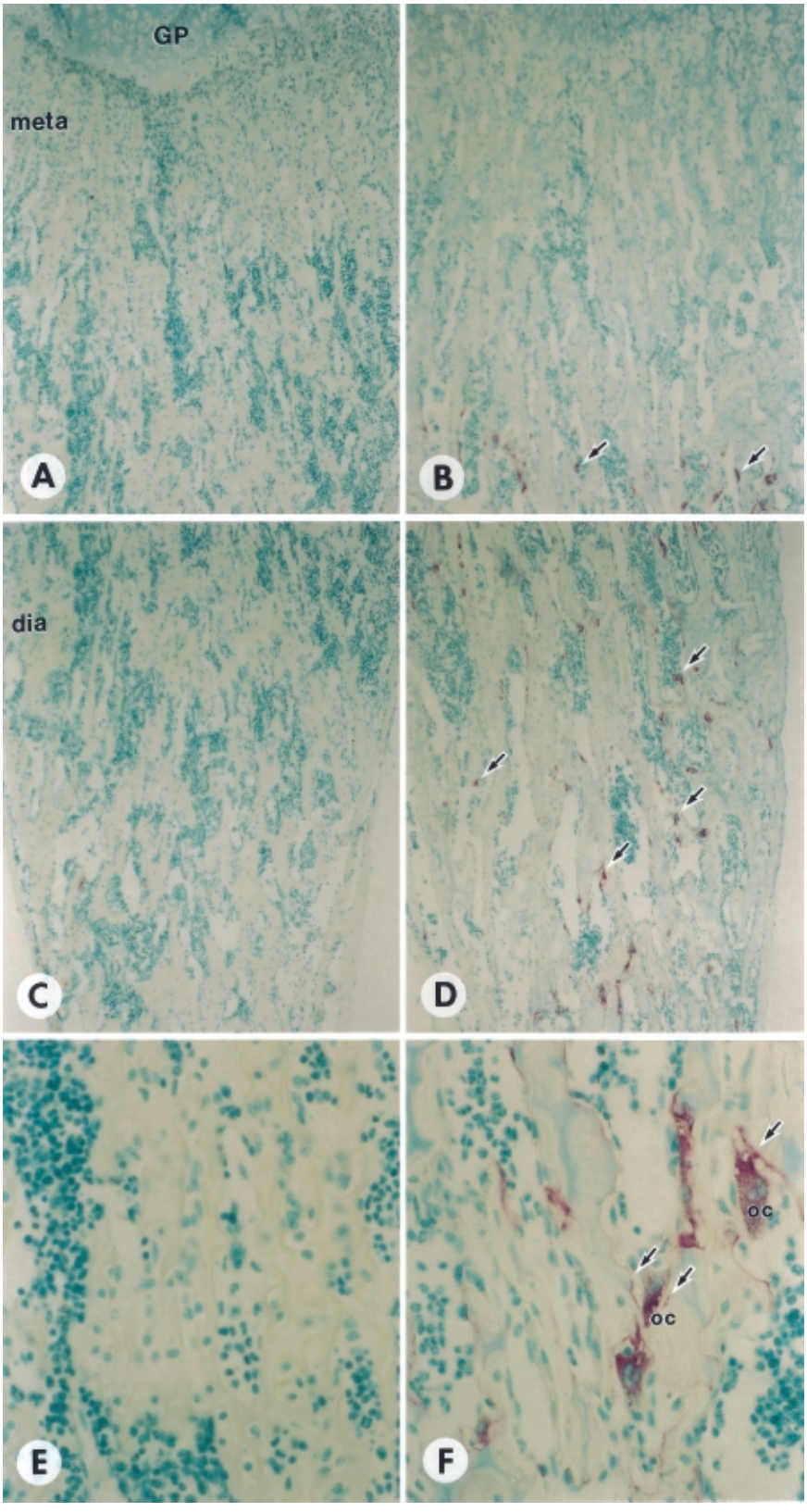

Fig. 1. Tartrate-resistant acid phosphatase (TRACPase) enzyme histochemistry of tibiae of op/op mice with (**B**, **D**, **F**) or without (**A**, **C**, **E**) macrophage colony-stimulating factor (M-CSF) injection. **A**, **B** Metaphyses (*meta*). **C**–**F** Diaphyses (*dia*). TRACPase-positive osteoclasts (arrows) can be seen in the diaphyseal region of tibiae in the M-CSF injected op/op mouse (**B**, **D**), whereas no TRACPase-positive osteoclasts were found in the control op/op mouse (**A**, **C**, **E**). At higher magnification, TRACPase-positive reversal lines (*arrows*) were observed continuing the resorption lacunae on which TRACPase-positive osteoclasts (*oc*) were located (**F**). *GP*, growth plate. ×70 (**A**–**D**), ×320 (**E**, **F**)

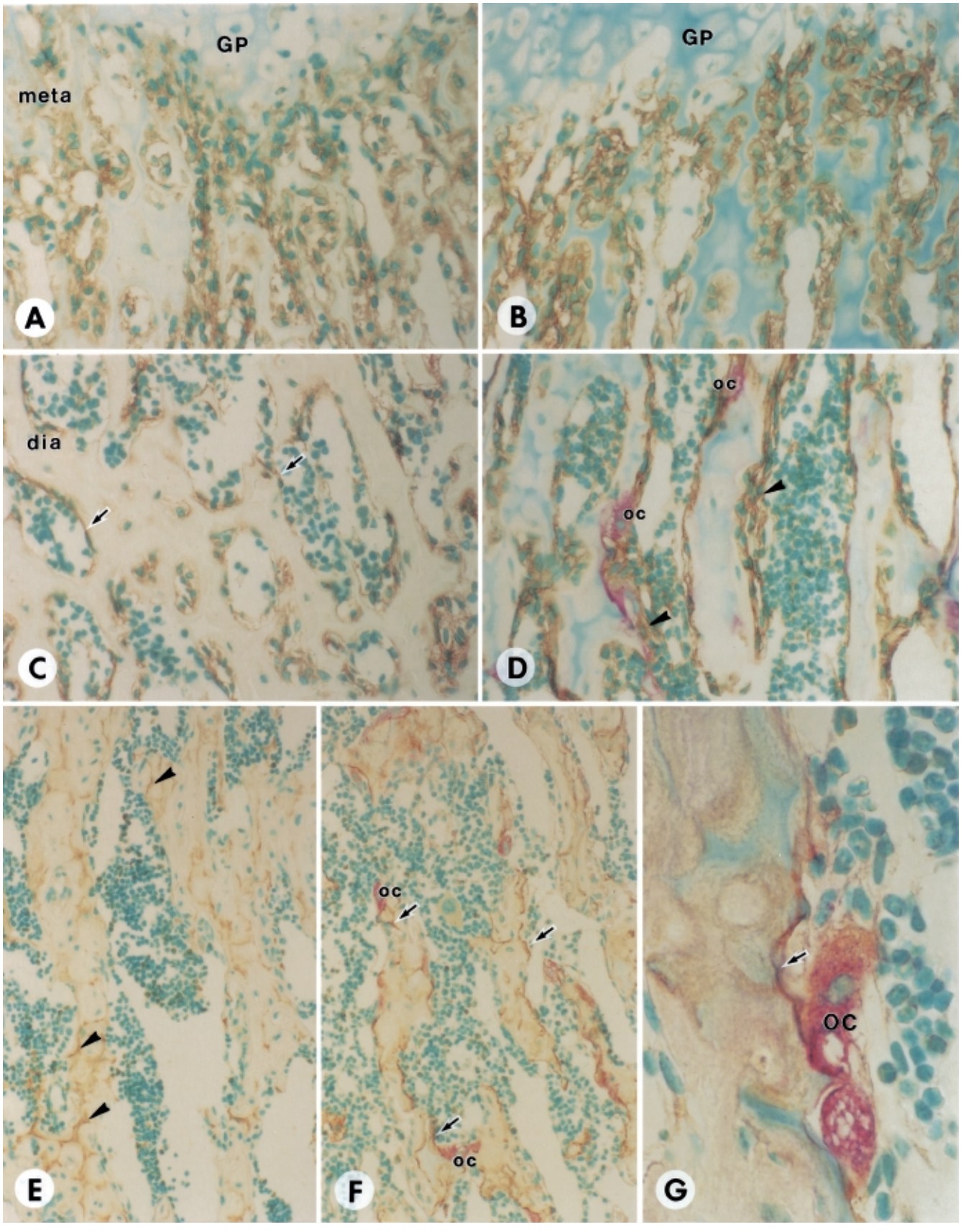
GP
meta
A
GP
B
dia
C
oc
oc
D
E
oc
oc
F
OC
G

Results

Appearance of TRACPase-positive osteoclasts

TRACPase histochemistry revealed no osteoclasts, cement lines or reversal lines in control op/op mice (Fig. 1A,C,E). Trabeculae, without any discontinuity, were elongated to the diaphysis from the chondro–osseous junction. A small amount of bone marrow tissue was observed between the trabeculae. However, 5 days after the injection of M-CSF, several TRACPase-positive osteoclasts appeared in the diaphysis (Fig. 1D), but not in the region of the metaphysis of the tibiae (Fig. 1B). TRACPase-positive reversal lines were observed to be continuing the resorption lacunae on which TRACPase-positive osteoclasts were located (Fig. 1F). Notably, 5 days after the injection, osteoclasts could not be observed in the region of the chondro–osseous junction reffered to as the erosion zone, in which terminal chondrocyte lacunae permit successive vascular invasion prior to osteoclastic resorption, resulting in the formation of the mineralized scaffolds of cartilage cores.

Histochemical examination of ALPase, TRACPase and OPN

Next, we examined ALPase-positive osteoblasts in tibiae from mice with or without M-CSF injection (Fig. 2). In the metaphysis of the tibiae of control op/op mice, especially at the erosion zone, a large number of cuboidal osteoblasts was observed on the primary trabeculae composed of cartilage and bone matricies (Fig. 2A). ALPase immunoreactivity was detected on the cell membrane of these osteoblasts (Fig. 2A). In contrast with the metaphysis, most diaphyseal osteoblasts in control op/op mice exhibited a flattened shape, in spite of ALPase positivity, thus resembling so-called bone-lining cells (Fig. 2C). OPN was observed faintly in the bone matrix, whereas OPN staining at the bone–cartilage interface of the trabeculae was intense (Fig. 2E).

Alternatively, after injection of M-CSF, diaphyseal osteoblasts were intensely positive for ALPase, and turned into cuboidal cells (Fig. 2D). TRACPase-positive osteoclasts located on the trabeculae showed a close association with these ALPase-positive osteoblasts, forming resorption lacunae positive for TRACPase (Fig. 2D). Intense OPN immunopositivity was found on the surface of trabecular bones where TRACPase-positive osteoclasts existed (Fig. 2F). When observed at a higher magnification, strong OPN immunoreactivity was seen to overlap TRACPase-positive resorption lacunae beneath osteoclasts (Fig. 2G). Compared with the histological changes seen in the diaphysis after injection of mice with M-CSF, the metaphysis did not exhibit any dynamic changes, particularly with respect to the osteoblasts (compare Fig. 2A and 2B).

Ultrastructural observations in op/op mice with or without injections of M-CSF

In the metaphysis of op/op mice, primary trabeculae, consisted of irregularly shaped cartilage core and bone matrix deposits (Fig. 3A). The interface between the cartilage and bone in the trabeculae was osmiophilic, indicating abundant organic components (Fig. 3B). An electron-dense linear structure identical to a cement line or reversal line was not evident in primary trabecular bones because of no osteoclastic bone resorption (Fig. 3A). Undecalcified sections demonstrated a large number of patchy calcified nodules, representing incomplete calcification of bone matrices (Fig. 3C). In contrast, in the diaphysis of op/op mice, electron microscopy revealed flattened osteoblasts located on the diaphyseal trabeculae (Fig. 4A).

In contrast with control op/op mice, their counterparts injected with M-CSF revealed osteoclasts characterized by multinuclei, many mithocondria and well-developed ruffled borders (Fig. 4B). Interestingly, osteoblasts in the vicinity of bone-resorbing osteoclasts were cuboidal, and appeared to be activated, as evidenced by ultrastructural features including well-developed Golgi apparatus and rough endoplasmic reticulum (rER). Electron-dense linear structures identical to cement lines or reversal lines were often observed underlying bone-resorbing osteoclasts, and were continuous from the resorption lacunae (Fig. 5A). Osteoblasts were located on and over the electron-dense linear structures, which were associated with the

Fig. 2. Double staining of alkaline phosphatase (ALPase)/TRACPase (**A**–**D**) and osteopontin (OPN)/TRACPase (**E**–**G**). The ALPase immunoreactivity was detected on cell membranes of metaphyseal (*meta*) osteoblasts in the op/op mouse injected with M-CSF (**B**), or not (**A**). In the diaphysis (*dia*), osteoblasts in the control op/op mouse were flattened (*arrows*), showing less-intense ALPase-positivity (**C**), while those treated with M-CSF exhibited strong ALPase reactivity (**D**). TRACPase-positive osteoclasts (*oc*) formed scallop-shaped resorption lacunae. Note the osteoblastic cell layer (*arrowheads* in **D**), which is thicker than that seen in the control op/op mouse (**C**). OPN was faintly seen in the bone matrix, and moderately at the bone–cartilage interface (*arrowheads*) of the trabeculae (**E**). Apparent OPN immunopositivity (*arrows*) was detected on the surfaces of the trabecular bones when injected with M-CSF (**F**). A higher magnification demonstrates OPN immunoreactivity (*arrow*) overlapping TRACPase-positive resorption lacunae (shown in red) beneath the osteoclasts (**G**). *GP*, growth plate. ×280 (**A**, **B**), ×130 (**E**, **F**), ×640 (**G**)

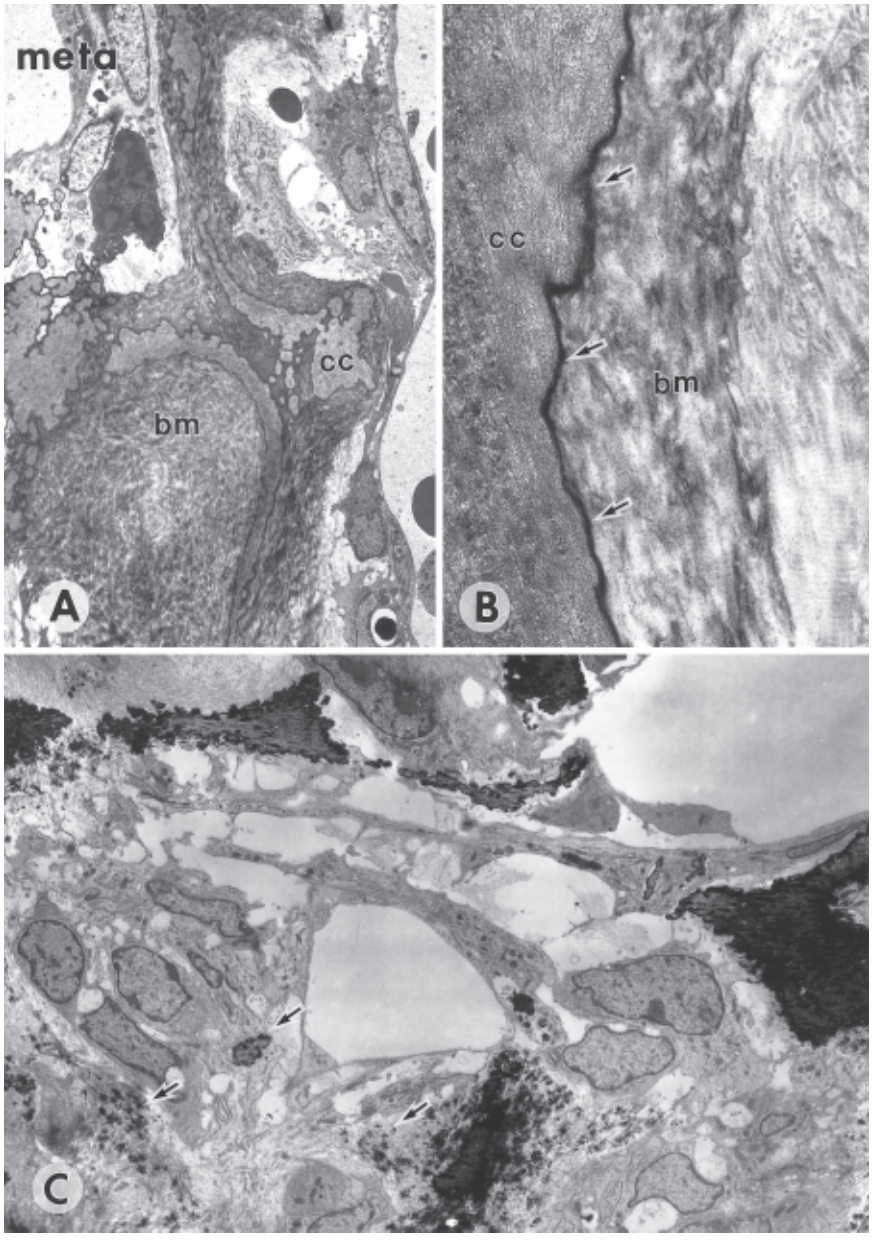

Fig. 3. The metaphysis of the op/op mouse consisted of an irregularly shaped cartilage core (*cc*) and bone matrix (*bm*) (**A**). Osmiophilic material (*arrows*) was found at the interface between the cartilage core (*cc*) and bone matrix (*bm*) (**B**). Undecalcified sections revealed scattered patches (*arrows*) of calcified nodules (**C**). *meta*, metaphysis; *dia*, diaphysis. ×1500 (**A**), ×41 000 (**B**), ×1800 (**C**)

ruffled borders of the osteoclasts (Fig. 5A). At a higher magnification, fibrillar but amorphous components were seen to be attached to the linear electron-dense structures, indicating newly deposited bone matrix towards the electron dense structures on the surface of the cartilage and bone (Fig. 5B).

Discussion

The present study demonstrated that osteoblasts at the erosion zone were not affected by the absence or presence of osteoclasts, and that, in contrast with metaphyseal osteoblasts, the activation of diaphyseal osteoblasts requires osteoclasts or osteoclastic bone resorption, which, therefore, indicates the existence of a "coupling factor," as predicted by Howard et al. [15].

The op/op mouse appears to be a good model in which to monitor the effects of M-CSF and consequent histological events. Morphological analysis for young op/op mice has been previously undertaken by Marks, who determined that osteoclasts are rare, small in size with unclear ruffled borders, and no resorption lacunae are observed on bone surfaces [33]. Bone growth in op/op mice basically depends on endochondral ossification by osteoblasts, despite there being no bone remodeling. Endochondral ossification is thought to occur at the erosion zone where osteoblasts deposit new bone ma-

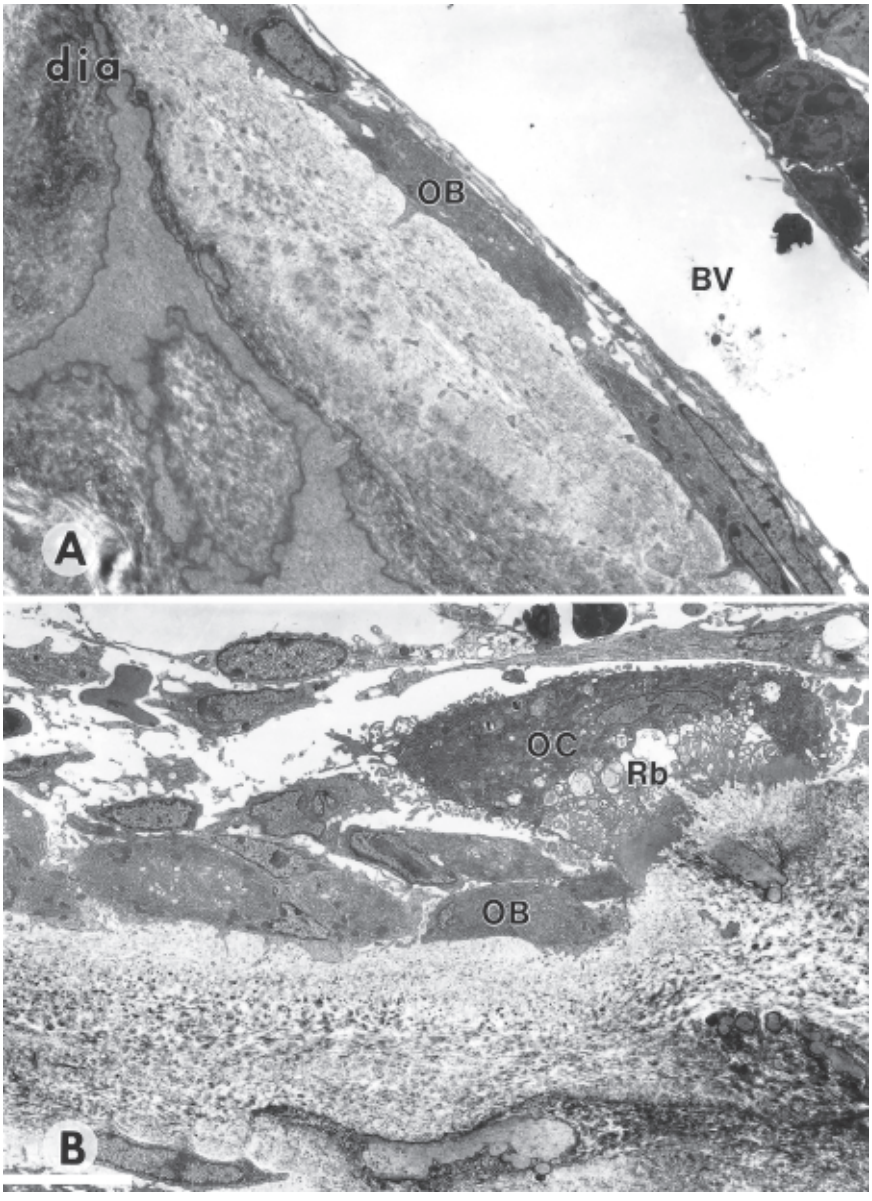

Fig. 4. Electron microscopic observations of the diaphyses (*dia*) of tibiae of op/op mice that were (**B**) or were not (**A**) injected with M-CSF. In the control animal (**A**), electron microscopy showed flattened osteoblasts (*OB*) located on the trabeculae. When injected with M-CSF (**B**), osteoblasts (*OB*) were cuboidal, and were characterized by well-developed Golgi apparatus and rough endoplasmic reticulum. Osteoclasts (*OC*) with multinuclei, many mitochondria and well-developed ruffled borders (*Rb*) were seen (**B**). *BV*, blood vessel. ×1800 (**A**), ×1500 (**B**)

trix onto calcified cartilage scaffolds. Although there were no osteoclasts in the erosion zone in op/op mice, the longitudinal cartilage scaffolds were formed. The formation of longitudinal trabeculae in op/op mice may be explained by cartilage matrix calcification parallel to the longitudinal axis [34], and the subsequent invasion of vascular endothelial cells and septoclast/perivascular cells into the transverse partitions of cartilage matrix in the hypertrophic zone [35–37]. In the metaphysis of op/op mice, the osteoblasts possessed well-developed Golgi apparatus and rER, showing strong ALPase immunoreactivity. It appears likely that metaphyseal osteoblasts are constitutively activated in op/op mice, resulting in well-formed trabeculae, and, therefore, the osteoblasts may be affected by factors other than the presence of osteoclasts, and these other factors may be derived from the hypertrophic chondrocytes, or from some local factors embedded in cartilage matrix.

After M-CSF injection to op/op mice, as previously reported by Sandquist et al. [38], osteoclasts appeared in the region of the diaphysis, but not in the metaphysis. Frequent induction of osteoclasts in the diaphysis appears to be due, in part, to the abundance of osteoclast precusors in bone marrow-rich diaphyseal regions rather than in the metaphysis, as proposed by Sundquist et al. [38] The diaphysis of op/op mice injected with M-CSF revealed prompt induction of bone remodeling caused by the formation of osteoclasts. Following M-

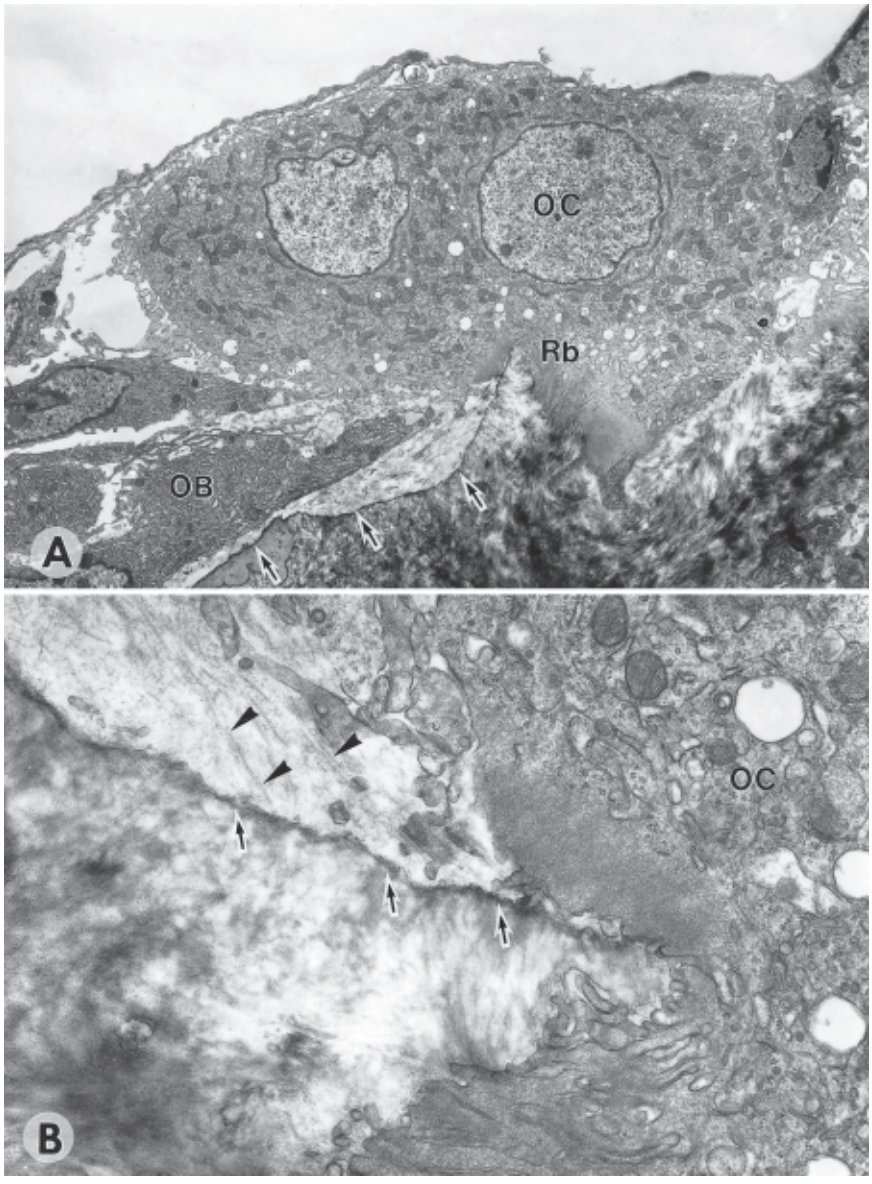

Fig. 5. Electron microscopic images of an osteoclast induced by M-CSF injection. An electron-dense linear structure (*arrows*) was seen on the surface continuing from the resorption lacuna where the bone-resorbing osteoclast (*OC*) is located (**A**). Note osteoblasts (*OB*) located on and over the linear electron-dense structure. At higher magnification, faintly stained fibrillar components (*arrowheads*) were scattered about, and some were associated with the linear elecron-dense structures (*arrows*) (**B**). *Rb*, ruffled border. ×2400 (**A**), ×22000 (**B**)

CSF injection, diaphyseal osteoblasts showed marked ALPase activity, and well-developed Golgi apparatus and rER, suggesting stimulated activity. Because osteoblasts do not possess the receptor for M-CSF [26,27,39], the activation of osteoblasts seems to be a consequence of the formation of osteoclasts or osteoclastic bone resorption. Based on our own observations, we support the idea of a "coupling factor", previously proposed by Howard et al. [15], which may be responsible for the shift from bone resorption to formation by acceleration of the activity of osteoblasts.

Although many researchers have suggested candidates for the coupling factor, including BMPs, TGF-β, insulin-like growth factor (IGF)-I, II, and OPN, the actual factor and its distribution have not yet been determined. A coupling factor appears to play an important role in the migration and attachment of osteoblastic cells to bone surfaces. Therefore, a coupling factor may exist in bone matrix, particularly on the reversal lines that are continuous to the resorption lacunae. BMPs and TGF-β belong to the same family and are distributed extensively in the bone matrix, and their ability to induce ectopic bone formation, probably caused by induction of osteoblastic differentiation, has been described previously [40–43]. Because TGF-β immunodistribution corresponding to cement lines has been reported by Hosoi et al. [44], the abundance of OPN in cement lines and the lamina limitans points to the possibility of its involvement in coupling. The finding that OPN immunoreactivity overlapped TRACPase-

positive resorption lacunae in M-CSF-injected op/op mice is supported by results of previous reports [17–19,45]. Based on electron microscopic observations, OPN immunopositivity on the resorption lacunae and reversal lines seems to be identical to the linear electron-dense structure of the trabeculae that was previously resorbed by osteoclasts. In addition, fibrillar components scattered throughout the elecron-dense structure indicate new bone formation by osteoblasts. Therefore, it is possible that OPN is significant for coupling in the reversal phase. However, it is well known that OPN is a multifunctional protein. OPN has been localized on calcified nodules [46–49] and on electron-dense lamina limitans [46–53], and binds strongly to hydroxyapatite [54]. In addition, OPN is chemotactic to macrophage lineages, possibly including osteoclasts [55], and binds osteoclast αvβ3 integrin through an RGD motif [16,56–59]. These reports indicate that OPN is involved in the migration and attachment of osteoclasts to bone surfaces. However, it does not seem contradictory that OPN acts for both osteoclastic migration/attachment and osteoblastic activity in the reversal phase.

In summary, the present study demonstrated that osteoblasts at the erosion zone appear to be less responsive to osteoclasts, and diaphyseal osteoblasts are affected by osteoclastic activity.

Acknowledgments. We thank Morinaga Milk for their kind provision of rhM-CSF, and Shin-ichi Kenmotsu for his invaluable assistance. This work was supported, in part, by funding from Kato Memorial Bioscience (N.A.).

References

1. Currey JD (1964) Three analogies to explain the mechanical properties of bone. Biorrheol 2:1–10
2. Curry JD (1969) The relationship between the stiffness and the mineral content of bone. J Biomech 2:477–480
3. Katz JL (1971) Hard tissue as a composite material. I. Bounds on the elastic behavior. J Biomech 4:455–473
4. Katz JL (1980) The structure and biomechanics of bone. In: Vincent JFV, Curry JD (eds) Mechanical Properties of Biological Materials. Cambridge University Press, Cambridge, pp 137–168
5. Baron R, Vignery A, Horowits M (1983) Lymphocytes, macrophages and the regulation of bone remodeling. In: Peck WA (ed.) Bone and Mineral Research, Annual 2. Elservier Science New York, pp 175–243
6. Miller SC, Bowman BM, Smith JM, Jee WSS (1980) Characterization of endosteal bone-lining cells from fatty marrow bone sites in adult beagles. Anat Rec 198:163–173
7. Burger EH, Van der Meer JWM, Nijweide PJ (1984) Osteoclast formation from mononuclear phagacytes: role of bone forming cells. J Cell Biol 99:1901–1906
8. Takahashi N, Yamana H, Yoshiki S, Roodman GD, Mundy GR, Jons SJ, Boyde A, Suda T (1988) Osteoclast-like cell formation and its regulation by osteotropic hormones in mouse bone marrow cultures. Endocrinology 122:1373–1382
9. Udagawa N, Takahashi N, Akatsu T, Sasaki T, Yamaguchi A, Kodama H, Martin TJ, Suda T (1989) The bone marrow-derived stromal cell lines NC3Ts-G2/PA6 and ST2 support osteoclast-like cell differentiation in cocultures with mouse spleen cells. Endocrinology 125:1805–1813
10. Yasuda H, Shima N, Nakagawa N, Yamaguchi K, Kinosaki M, Mochizuki S, Tomoyasu A, Yano K, Goto M, Murakami A, Tsuda E, Morinaga T, Higashio K, Udagawa N, Takahashi N, Suda T (1998) Osteoclast differentiation factor is a ligand for osteoprotegerin/osteoclast inhibitory factor and is identical to TRANCE/RANKL. Proc Natl Acad Sci USA 95:3597–3602
11. Baron R, Neff L, Louvard D, Courtoy P (1985) Cell-mediated extracellular acidification and bone resorption: evidence for a low pH in resorbing lacunae and localization of a 100-kD lysosomal memblane protein at the osteoclast ruffled border. J Cell Biol 101:2210–2222
12. Oguro I, Ozawa H (1988) The histochemical localization of acid phosphatase activity in BMU. J Bone Miner Metab 6:45–49
13. Frost HM (1964) Dynamics of bone remodeling. In: Frost HM (ed.) Bone Biodynamics. Little Brown, Boston, pp 315–333
14. Wergedal J, Baylink DJ (1969) Distribution of acid and alkaline phosphatase activity in undemineralized sections of the rat tibial diaphysis. J Histochem Cytochem 17:799–806
15. Howard GA, Bottemiller BL, Turner RT, Rader JI, Baylink DJ (1981) Parathyroid hormone stimulates bone formation and resorption in organ culture: evidence for a coupling mechanism. Proc Natl Acad Sci USA 78:3204–3208
16. Flores M, Norgard M, Heinegard D, Reinholt F, Andersson G (1992) RGD-directed attachment of isolated rat osteoclasts to osteopontin, bine sialoprotein and fibronectin. Exp Cell Res 201:526–530
17. Merry K, Dodds R, LittleWood A, Gowen M (1993) Expression of osteopontin mRNA by osteoclasts and osteoblasts in modelling adult human bone. J Cell Sci 104:1013–1020
18. Dodds RA, Connor JR, James IE, Lee Rykaczewski E, Appelbaum E, Dul E, Gowen M (1995) Human osteoclasts, not osteoblasts, deposit osteopontin onto resorption surfaces: an in vitro and ex vivo study of remodeling bone. J Bone Miner Res 10:1666–1679
19. Arai N, Ohya K, Ogura H (1993) Osteoponton mRNA expression during bone resorption: an in situ hybridization study of induced ectopic bone in the rat. Bone Miner 22:129–145
20. Yamate T, Mocharla H, Taguchi Y, Igietseme JU, Manolagas SC, Abe E (1997) Osteopontin expression by osteoclast and osteoblast progenitors in the murine bone marrow: demonstration of its requirement for osteoclastgenesis and its increase after ovariectomy. Endocrinology 138:3047–3055
21. Wiktor-Jedrzejczak WW, Ahmed A, Szezylik C, Skelly RR (1982) Hematological characterization of congenital osteopetrosis in op/op mouse. Possible mechanism for macrophage differentiation. J Exp Med 156:1516–1527
22. Wiktor-Jedrzejczak W, Urbanowska E, Aukerman SL, Pollard JW, Stanley ER, Ralph P, Ansari AA, Sell KW, Szpirl M (1991) Correction by CSF-1 of defects in the osteopetrotic op/op mouse suggests local, developmental, and humoral requirements for this growth factor. Exp Hematol 19:1049–1054
23. Yoshida H, Hayashi S, Kunisada T, Ogawa M, Nishikawa S, Okamura H, Sudo T, Shultz LD, Noshikawa S (1990) The murine mutation osteopetrosis is in the coding region of the macrophage colony stimulating factor gene. Nature 345:442–444
24. Takahashi N, Udagawa N, Akatsu T, Tanaka H, Isogai Y, Suda T (1991) Deficiency of osteoclasts in osteopetrotic mice is due to a defect in the local microenvironment provided by osteoblastic cells. Endocrinology 128:1792–1796
25. Felix R, Cecchini MG, Fleisch H (1990) Macrophage colony-stimulating factor restores in vivo bone resorption in the op/op mouse. Endcrinology 127:2592–2594
26. Kodama H, Yamasaki A, Nose M, Niida S, Ohgame Y, Abe M, Kumegawa M, Suda T (1991) Congenital osteoclast deficiency in

osteopetrotic (op/op) mice is cured by injections of macrophage colony-stimulating factor. J Exp Med 173:269–272
27. Kodama H, Nose M, Niida S, Yamasaki A (1991) Essential role of macrophage colony-stimulating factor in the osteoclast differentiation supported by stromal cells. J Exp Med 173:1291–1294
28. Niida S, Amizuka N, Hara F, Ozawa H, Kodama H (1994) Expression of Mac-2 antigen in the preosteoclast and osteoclast identified in the op/op mice injected with macrophage colony-stimulating factor. J Bone Miner Res 9:873–881
29. Marks SC Jr., Lane PW (1976) Osteopetrosis, a new recessive skeletal mutation on chromosome 12 of the mouse. J Hered 67: 11–18
30. Amizuka N, Yamada M, Watanabe J, Hoshi K, Fukushi M, Oda K, Ikehara Y, Ozawa H (1998) Morphological examination of bone synthesis via direct administration of basic fibroblast growth factor into rat bone marrow. Microsc Res Tech 41:313–322
31. Oldberg A, Franzen A, Heinegard D (1986) Cloning and sequence analysis of rat bone sialoprotein (osteopontin) cDNA reveals an Arg-Gly-Asp cell-binding sequence. Proc Natl Acad Sci USA 83:8819–8823
32. Amizuka N, Takahashi N, Udagawa N, Suda T, Ozawa H (1997) An ultrastructural study of cell–cell contact between mouse spleen cells and calvaria-derived osteoblastic cells in a co-culture system for psteoclast formation. Acta Histochem Cytochem 30: 351–362
33. Marks SC Jr (1982) Morphological evidence of reduced bone resorption in osteopetrotic (op) mouse. J Anat 163:157–167
34. Sasaki T, Amizuka N, Irie K, Ejiri S, Ozawa H (2000) Localization of alkaline phosphatase and osteopontin during mineralization in developing cartilage of caudal vertebrae. Arch Histol Cytol 63:271–284
35. Hunter GK, Kyle CL, Goldberg HA (1994) Modulation of crystal formation by bone phosphoproteins: structural specificity of the osteopontin-mediated inhibition of hydroxyapatite formation. Biochem J 300:723–728
36. Lee ER, Lamplugh L, Shepard NL, Mort JS (1995) The septoclast, a cathepsin B-rich cell involved in the resorption of growth plate cartilage. J Histochem Cytochem. 43:525–536
37. Nakamura H, Ozawa H (1996) Cell–cell and cell matrix interaction in bone remodeling. J Jpn Orthop Assoc 70:14–24
38. Sundquist KT, Cecchini MG, Marks SC Jr (1995) Colony-stimulating factor-1 injections improve but do not cure skeletal sclerosis in osteopetrotic (op) mice. Bone 16:39–46
39. Niida S, Abe M, Suemune S, Yoshiko Y, Maeda N, Yamasaki A (1997) Restoration of disturbed tooth eruption in osteopetorotic (op/op) mice by injection of macrophage colony-stimulating factor. Exp Anim 46:95–101
40. Bentz H, Nathan PM, Rosen DM, Armstrong RM, Thompson AY, Segarini PR, Mathews MC, Dasch JR, Piez KA, Seyedin SM (1989) Purification and characterization of a unique osteoinductive factor from bovine bone. J Biol Chem 264:20805–20810
41. Urist MR (1965) Bone formation by autoinduction. Science 150:893–899
42. Urist MR, Iwata H, Cecotti PL, Dorfman RL, Boyd SD, McDowell RM, Chien C (1973) Bone morphogenesis in implants of insoluble bone gelatin. Proc Natl Acad Sci USA 70:3511–3515
43. Wozney JM, Rosen V, Celeste AJ, Mitsock LM, Whitters MJ, Kriz RW, Hewick RM, Wang EA (1998) Novel regulators of bone formation: molecular clones and activities. Science 242:1528–1534
44. Hosoi T, Asaka T, Motoo M, Tomita T, Shiraki M, Inoue S, Ouchi Y, Orimo H (1996) Immunolocalization of transforming growth factor-β in the bone tissue. Calcif Tissue Int 59:305–306
45. Ek-Rylander B, Flores M, Wendel M, Heinegard D, Andersson G (1994) Dephosphorylation of osteopontin and bone sialoprotein by osteoclastic tartrate-resistant acid phosphatase. J Biol Chem 269:14853–14856
46. McKee MD, Nanci A (1990) Ultrastructural, cytochemical and immunocytochemical studies on bone and its interfaces. Cells Materials 3:219–243
47. McKee MD, Nanci A, Landis WJ, Gotoh Y, Gerstenfeld LC, Glimcher MJ (1990) Developmental appearance and ultrastructural immunolocalization of a major 66 kD phosphoprotein in embryonic and post-natal chicken bone. Anat Rec 228:77–92
48. McKee MD, Glimcher MJ, Nanci A (1992) High-resolution immunolocalization of osteopontin and osteocalcin in bone and cartilage during endochondral ossification in the chicken tibia. Anat Rec 234:479–492
49. McKee MD, Farach CM, Butler WT, Hauschka PV, Nanci A (1993) Ultrastructural immunolocalization of noncollagenous (osteopontin and osteocalcin) and plasma (albumin and alpha 2HS-glycoprotein) proteins in rat bone. J Bone Miner Res 8:485–496
50. Scherft JP (1972) The lamina limitans of the organic matrix of calcified cartilage and bone. J Ultrastruct Res 38:318–331
51. Scherft JP (1978) The lamina limitans of the organic bone matrix: formation in vitro. J Ultrastruct Res 64:173–181
52. Hultenby K, Reinholt FP, Oldberg A, Heinegard D (1991) Ultrastructural immunolocalization of osteopontin in metaphyseal and cortical bone. Matrix 11:206–213
53. Hultenby K, Reineholt F, Norgard M, Oldberg A, Wendel M, Heinegard D (1994) Distribution and synthesis of bone sialoprotein in metaphyseal bone of young rats show a distinctly different pattern from that of osteopontin. Eur J Cell Biol 63:230–239
54. Franzen A, Heinegard D (1985) Isolation and characterization of two sialoproteins present only in bone calcified matrix. Biochem J 232:715–724
55. Kaneto H, Morrissey J, McCracken R, Reyes A, Klahr S (1998) Osteopontin expression in the kidney during unilateral ureteral obstruction. Miner Electrolyte Metab 24:227–237
56. Reinholt FP, Hultenby K, Oldberg A, Heinegard D (1990) Osteopontin: a possible anchor of osteoclasts to bone. Proc Natl Acad Sci USA 87:4473–4475
57. Miyauchi A, Alvarez J, Greenfield EM, Teti A, Grano M, Colucci S, Zambonin-Zallone A, Ross FP, Teitelbaum SL, Cheresh D, Hruska KA (1993) Binding of osteopontin to the osteoclast αvβ3 integrin. Osteoporosis Int 1:132–135
58. Ross FP, Chappel J, Alvarez JI, Sander D, Butler WT, Farach CM, Mintz KA, Robey PG, Teitelbaum SL, Cheresh DA (1993) Interactions between the bone matrix proteins osteopontin and bone sialoprotein and the osteoclast integrin alpha v beta 3 potentiate bone resorption. J Biol Chem 268:9901–9907
59. Faccio R, Grano M, Colucci S, Zambonin-Zallone A, Quaranta V, Pelletier AJ (1998) Activation of αvβ3 integrin on human osteoclast-like cells stimulates adhesion and migration in response to osteopontin. Biochem Biophys Res Commun 249:522–525